ANALYSIS OF HIERARCHICAL CONTROL IN A DC MICROGRID WITH DROOP STRATEGY APPLIED TO A FRONT-END DC-AC CONVERTER TO REGULATE DC BUS VOLTAGE

MARCELLO NEVES*, MATHEUS SOARES*, FELIPE DICLER*, MAURÍCIO AREDES*

*Laboratório de Eletrônica de Potência e Média Tensão – LEMT
Universidade Federal do Rio de Janeiro – UFRJ
Rio de Janeiro, RJ, Brasil

E-mails: marcello@lemt.ufrj.br, matheussoares@lemt.ufrj.br, dicler@lemt.ufrj.br, aredes@lemt.ufrj.br

Abstract— This work investigates the influence of a droop control approach implemented to a front-end DC-AC converter connected to a DC microgrid. Distributed energy systems operating in a DC microgrid structure have been gaining traction recently, mainly due to the simplification process in the integration of renewable generation and energy storage systems. One of the most common strategies to guarantee proper operation of these structures is the droop control, which presents relatively easy implementation, enables microgrid coordination and also DC bus voltage regulation. However, the droop method lacks robustness and can present errors when lines between the terminals have non negligible impedances. This drawback can be mitigated with hierarchical control topologies. In addition to the aforementioned strategies, front-end DC-AC converters are also capable of contributing with DC bus voltage regulation if provided with proper droop strategy. To the best of the authors knowledge, this type of control has not been thoroughly explored, though. To partially fill this gap, the authors implemented a DC microgrid model in software environment, considering line cable impedances between units. In the front-end converter, the droop strategy is employed using the synchronous reference frame technique. Simulation results are presented to illustrate the influence of the control developed for the front-end converter in the performance of the microgrid, focusing on the primary and secondary responses. A comparison with the operation regimen under the most common control approach found in literature is also reported.

Keywords— Hierarchical Control, Droop Control, DC microgrids, Smart Grids.

1 Introduction

In the last decades, the utilization of renewable energies in the electric system has increased significantly, reducing pollution and the emission of CO2. Alternative sources, such as wind turbines, fuel cells and photovoltaic panels have been contributing with system generation within different levels of power in the utility grid, like transmission and distribution systems.

As a consequence, the distribution system has passed through several changes. A system which previously had only electric loads, nowadays has also distributed generation (DG) units that can be allocated and coordinated by the local consumers. The DGs increase the reliability and flexibility of the system, since these units can sustain the loads and contribute to the power quality in the grid. Active and autonomous distributed systems, called microgrids (MGs), aim to establish a more efficient energy system using energy storage (ES) units and robust control strategies.

In this scenario, the combination of DC based generation and ES units in a DC microgrid can improve the efficiency, and has some advantages (Dragicevic et al., 2016), such as:

- Reduction of power losses caused by the lower number of conversion steps;
- Most DGs, energy storage systems (ESS) based in batteries, and electronic loads have dc operation, so the integration becomes easier;
- The interconnection between systems or elements is much simpler than in AC, because the synchronization depends only on the DC voltage level;
- There is no reactive power in a DC MG. This fact simplifies the control strategies and improves power quality.

However, the coordination and energy management in DC MGs have some challenges that involve mainly voltage regulation at terminal connections and power sharing accuracy between generation and storage units. To achieve the aforementioned goals, several control strategies were proposed before (Ott et al., 2015). These strategies are very robust but they can lose accuracy depending on the system configuration and line impedances.

Besides the control methods, another relevant aspect in microgrids management is the communication between converters that interface the DGs and ESs components. Communication channels allow implementation of more sophisticated strategies and additional features. As a result, many works propose new types of controls and algorithms that have various purposes.

A control architecture applied to ESSs was already implemented. In (Xiao et al., 2015), a strategy that performs voltage regulation and autonomous state of charge (SoC) recovery is shown. In (Jin et al., 2014), a practical DC microgrid developed using only DC-DC converters is presented. These concepts can be expanded to other types of sources and converter topologies.

This paper aims to analyze a multilevel control method to manage DC microgrid equipment considering the effect of line impedances and a front-end DC-AC converter, where the control structure is adapted to regulate the DC bus voltage and to work with the hierarchical topology. The microgrid analyzed for the work is shown in Figure 1.

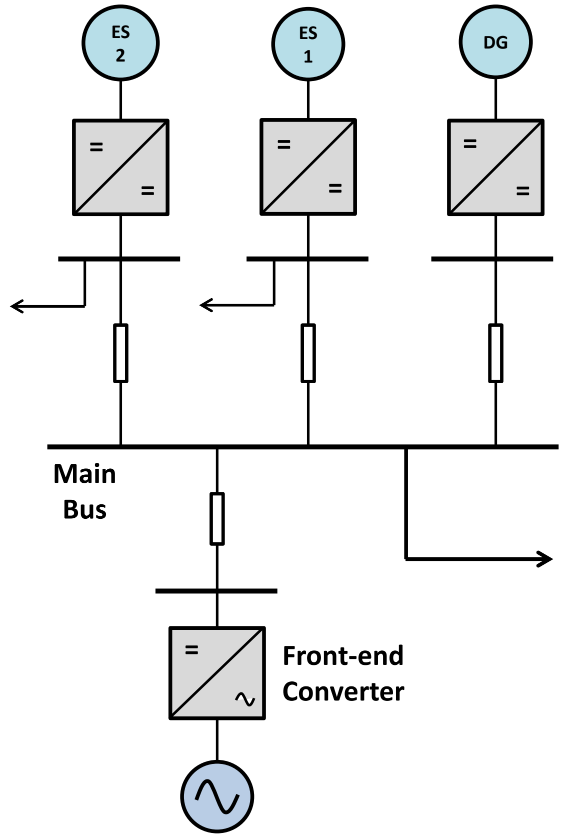

Figure 1. DC Microgrid Topology.

The system consists of a solar DG unit, two ESS converters, and an AC/DC converter connecting the main DC bus of the microgrid with the utility grid. Each converter terminal supplies linear resistive local loads, while in the main bus a constant power load is connected. The equipment terminals are integrated to the main bus through transmission lines, and their impedances are considered in the study. The main function of the hierarchical control is to regulate the main bus voltage and improve accuracy in the power sharing.

This paper is organized as follows. The hierarchical concepts and techniques are shown in section 2. The component description of the microgrid and how the hierarchical control was implemented is presented in section 3. Section 4 demonstrates the theories with the simulation results. Finally, conclusions are made in section 5.

2 Hierarchical Control

2.1 Topology

The hierarchical control topology is shown in Figure 2. Each converter unit connected to the system has a primary controller actuator, which processes the variables through local current and voltage measures. This means that primary controllers are able to work autonomously and regardless of a common communication channel.

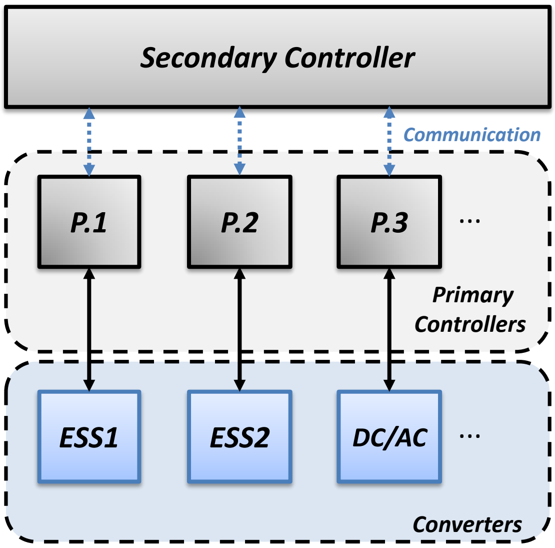

Figure 2. Hierarchical control topology.

However, recent progress in communication technologies and information enables the possibility of new features in control and management in some applications. As a consequence, functions provided by sophisticated algorithms that perform the optimization of the microgrid are progressively implemented (Meng et al., 2017). This is possible due to the fact that system variables are shared, avoiding mismatch errors and providing better decision making.

Nowadays, micrgrids complexity is growing, and the control must be realized in a smarter way. A hierarchical control structure is thus widely recommended. Simple functions can be implemented in the local controllers to guarantee a basic operation of the system. Advanced control and operational features can be implemented in a central controller. Hierarchical control is thus becoming a standardized configuration in microgrids. The secondary functions are conventionally performed in a centralized manner as they require global information, monitoring the main variables.

2.2 Primary control

The control in DC microgrids has many relevant tasks and aspects. Firstly, to guarantee the load supply, each converter must contribute with the power flow in the system proportional to its rated power capability. At the same time, the DC bus voltage must be monitored and has to operate near its nominal value. In this way the most common and practical control structure is the droop control.

The droop control scheme can be seen in the figure 3. The cascade control structure has the inductor current control as an inner loop. The outer loop is the terminal voltage control, which exports a current reference to the inner loop current control. Both controllers are based on Proportional-Integral (PI) controllers, with a transfer function described as:

$$G_{PI}(s) = K_p + \frac{1}{T_i s} \quad (1)$$

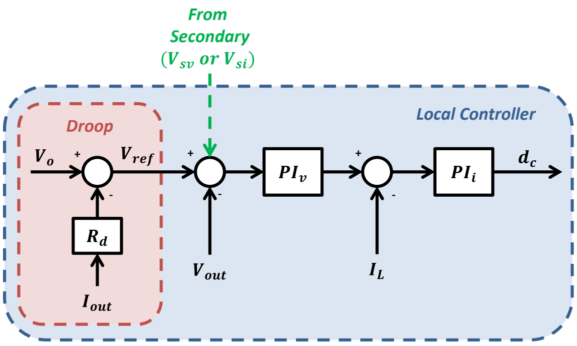

Figure 3. Primary control structure.

The droop strategy has the function to send a voltage reference to the local controller. This behavior provides the converters with the ability to control the bus voltage near its nominal value. Moreover, the power inserted by the interfaced converter in the microgrid is proportional to its rated power. These functions of the droop control can be seen through the droop equation below:

$$V_{ref} = V_0 - R_d I_{out} \quad (2)$$

where V_{ref} is the voltage reference sent to the outer loop, V_0 is the no-load voltage, I_{out} is the output current of the converter and R_d is the droop coefficient. It can be observed that the equation (2) makes the converter behave as a voltage source with a series resistance, since the droop coefficient has a resistive dimension. It means that this coefficient can be interpreted as a virtual resistance in the control, which causes a voltage droop in the voltage reference in steady state depending on the output current. With the droop method, converters in the MG work as slack terminals. The droop coefficient is calculated as follows:

$$R_d = \frac{V_{max} - V_{min}}{I_{max} - I_{min}} = \frac{\Delta V}{\Delta I} \quad (3)$$

Where ΔV is the maximum voltage variation allowed in the main dc bus of the microgrid and I_{max} the maximum output current of the converter. The droop control action is illustrated in the next figure. Droop curves can be different depending on the type of the converter and the type of element that is connected in to its input. Solar panels usually are unidirectional, so the converter only works inserting energy in the system.

In this case, the blue curve is used. ESSs can act in the system as a generation or as a load, and its interface converter must be bidirectional in current, following the green curve behavior. The utility grid converter does the interchange between grids and also can insert or absorb power into the microgrid.

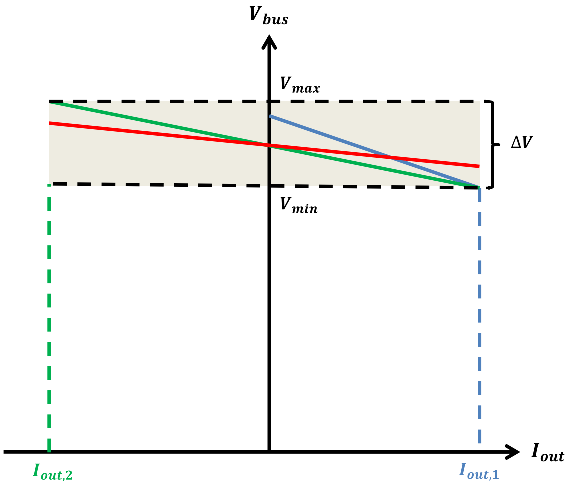

Figure 4 - Types of droop curves

It can be seen that the voltage dynamics in the microgrid is a result of all slack terminals variation. It is possible to deduce an equivalent droop curve from the droop curves parameters, illustrated by the red curve in the figure above. The incremental reaction of each droop curve in the system can be obtained deriving the equation. Hence:

$$\Delta I_n = -\frac{\Delta V}{R_{d,n}} \quad (4)$$

Where ΔI_n is the current variation on each converter. Therefore, the variation of all currents in the microgrid shows the variation of the whole system. Consequently:

$$\Delta I_{grid} = \sum_{n=1}^{k} \Delta I_n = -\Delta V \sum_{n=1}^{k} \frac{1}{R_{d,n}} \quad (5)$$

In the equation above, the voltage variation of each output converter is the same in the entire system, and is the previous stipulated ΔV_{max}. Manipulating the terms in the equation above, the expression of the equivalent droop coefficient of the microgrid is:

$$R_{eq} = \frac{-\Delta V}{\Delta I_{grid}} = \left(\sum_{n=1}^{k} \frac{1}{R_{d,n}} \right)^{-1} \quad (6)$$

Accordingly with the expression, it is possible to describe the relationship between main bus voltage value and the sum of all load currents connected to the system, which is:

$$V_{bus} = V_n - R_{eq} I_{load} \quad (7)$$

Where V_{bus} is the voltage measured in the main bus of the dc microgrid, V_n is the nominal value of the bus voltage, and I_{load} is the total load current linked at the main bus. As a result, the system can be treated as a single voltage source or slack terminal, with series equivalent virtual impedance. In fact, the equation (6) shows that the equivalent virtual resistance is the equivalent droop coefficient of the slack terminal based control converters, connected in parallel with the microgrid bus.

It is relevant to emphasize that some generation unit into the microgrid can work only as a constant power source, like MPPT based algorithms. To represent this equipment in the system, it is considered that their output current is constant and the effective load current is:

$$I'_{load} = I_{load} - \sum_{n=1}^{k} I_{DG,n} \tag{8}$$

Where I'_{load} is the effective load current used to calculate the voltage in equation (7), I_{load} is the total load current connected to main bus, and $I_{DG,i}$ is the current of DG unit.

The droop curves provide high flexibility due to the fact that many elements in the system can operate as a voltage slack terminal in the microgrid, regulating the main bus voltage between maximum and minimum values. Additionally, droop control improves the stability of the system because it can work without a communication channel. Each local controller uses the output current measured in the converter as information about the system load.

Unfortunately, droop control as a global method of control in the system is not enough to guarantee its optimal operation. The equation (7) indicates that the system will work with a steady state error in the voltage bus, because of the virtual impedance. Then the voltage regulation zone should be very small to minimize this phenomenon. Even more, this method can lose accuracy in power sharing due to real resistances between the converter terminal and the main bus (Chen et al., 2014), (Chen et al., 2015), (Iravani et al., 2016). The line resistances increase the voltage drop in to voltage regulation and cause power mismatches at the proportional power sharing, as illustrated in Figure 5.

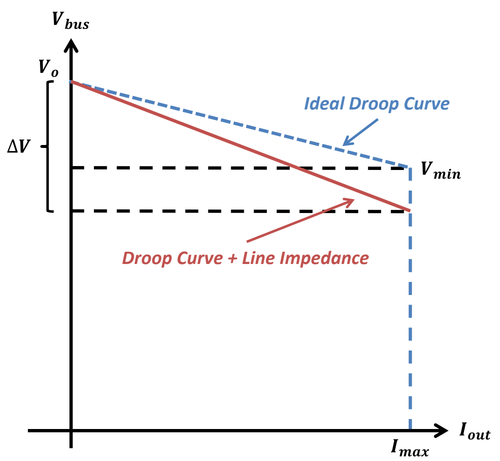

Figure 5. Line impedance effect in the droop behavior.

The droop equation considering the line impedances can be expressed as:

$$V_{ref} = V_0 - (R_d + R_{line})\, I_{out} \tag{9}$$

All variables in the equation above are the same in the equation (2). The only difference is the parameter R_{line} that represents the line impedance connected with the converter. In a dc distribution system, the resistance term of the impedance is most relevant because the dynamics caused by the impedances do not affect the steady state operation. It can be noted that the voltage regulation is harmed by the line impedance effect, since the minimum value of the bus voltage is violated. Line impedances also deteriorate the system power sharing, because the droop coefficient defined in the control is not the same as the effective series resistance.

2.2 Secondary Control

In large ac power systems, the concept of the secondary control is defined as the algorithms that correct the steady state error of system voltage and frequency. Similar principle is being used in dc microgrid control methodologies. For this specific study the secondary control will be used to eliminate the voltage deviation caused by the droop curves property. Besides, the secondary control can provide accuracy in the current sharing. The Figure 6 shows the control architecture.

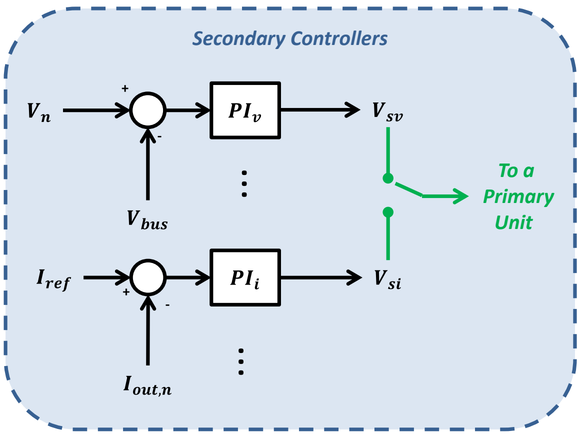

Figure 6. Secondary control scheme.

The two types of secondary control functions studied in this work are based on PI controllers, and both process the same variable output to the primary controller. However, they have different purposes and their action characterizes a tradeoff. Figure 7 analyzes this phenomenon.

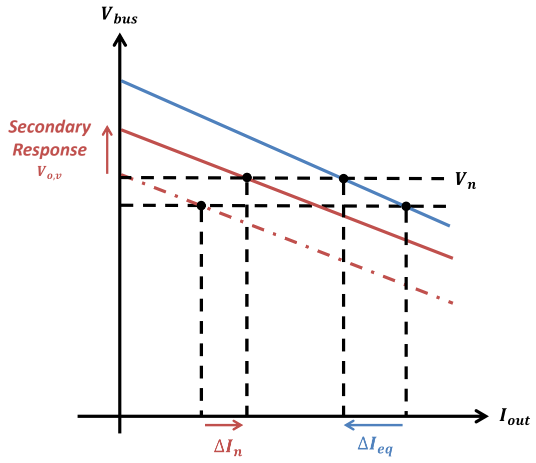

Figure 7. Secondary voltage regulation effect.

The figure above demonstrates the secondary action. The red curve is a converter with secondary action and the blue one is the equivalent of the other slack terminals in the MG. With a voltage variation on the V_{bus} axis, the droop curve suffers a shift. This voltage shift changes the operation point of the system and brings it to the point of the nominal voltage V_n. At this point, the secondary converter makes the output current rise. This rise causes power mismatches in presence of line impedances, because the voltage shift will be different since the other line impedances in other converters are distinct.

The current sharing compensation is done by the same effect. However, this voltage shift will cause a voltage deviation in the system bus, as it can be seen in Figure 8.

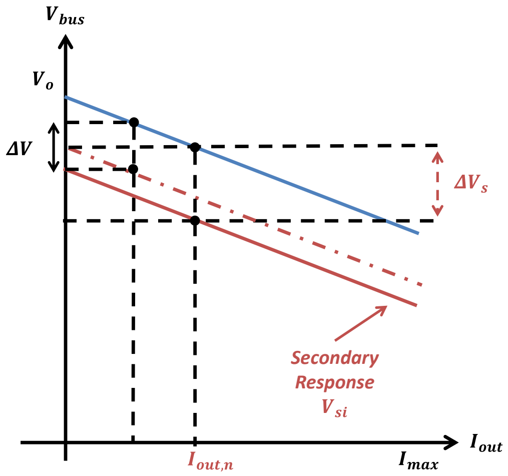

Figure 8. Secondary current compensation effect.

With the secondary response effect the difference of the terminal voltage of the converter is modified to achieve the accurate value of current. Therefore, it is not possible to achieve nominal voltage operation and perfect power sharing at the same time.

The voltage regulation of the secondary control is realized including a voltage shift in the droop equation. Hence:

$$V_{ref} = V_0 - R_d I_{out} + V_{sv} \tag{10}$$

Similarly, the current compensation is determined with:

$$V_{ref} = V_0 - R_d I_{out} + V_{si} \tag{11}$$

The equation that calculates the accurate output current of a converter is derived from the manipulation of equation (2) and substituting the voltage reference V_{ref} for the main bus voltage measured V_{bus}:

$$I_{out,n} = \frac{V_{bus} - V_0}{R_d} \tag{12}$$

3 Microgrid Components

This section describes the system simulated on PSCAD software to validate the theoretical aspects approached in this paper. The whole system was previously shown in Figure 1. Table 1 summarizes all the pertinent parameters of the microgrid components. The main bus of the microgrid operates with nominal value of 450 V, with a 10% of tolerance for maximum and minimum values for the primary controllers.

Table 1. Microgrid Parameters.

Converter	Input rms Voltage (V)	Rated Power (kW)	Line Impedance (Ω)	Local Resistive Loads (Ω)
DG	280.0	12.0	0.15	---
ESS1	240.0	12.0	0.10	20
ESS2	200.0	12.0	0.15	30
DC/AC	220.0 (ac side)	15.0	0.08	---

In the next items the details of modelling are described for each converter. The line impedances were chosen taken into account the characteristics of the cooper cables usually employed in power systems (Chen et al., 2014).

3.1 DG Unit

The DG unit consists of a photovoltaic array connected to the system through a unidirectional boost converter. Its controller aims to generate the maximum amount of power given the weather conditions. This type of control is commonly known in the literature as maximum power point tracking (MPPT). There are many techniques to apply the MPPT feature when the converter is connected in a microgrid (Zheng et al., 2011).

In this case, the incremental conductance algorithm was applied to process the MPPT capability on the DG unit.

3.2 ESS Units

There are two ESS distinct units which work individually, since both have their own interfacing converter. The control structure of the primary controllers is the same as the Figure 3. Nevertheless, the secondary control features have different objectives: Secondary performs voltage regulation with ESS1 and state of charge compensation in ESS2.

The state of charge methodology adopted to the simulation was elaborated accordingly to (Tremblay et al., 2007).

3.3 Front-end Converter

The front end converter is a bi-directional three phase DC/AC converter, which controls the power flow between DC microgrid and AC utility grid. The primary control strategy has to be adapted in this converter, whereas the inductors currents are in the ac side (Prieto-Araujo et al., 2017). To circumvent this situation, it was used the synchronous reference control frame, that transforms the three phase quantities in to stationary variables. With this technique, it is possible to use the PI controllers in d and q axis, and analogize the primary control of this converter with the control illustrated in Figure 3. The secondary control of this converter tends to regulate the main bus voltage. The control diagram applied is shown in Figure 9.

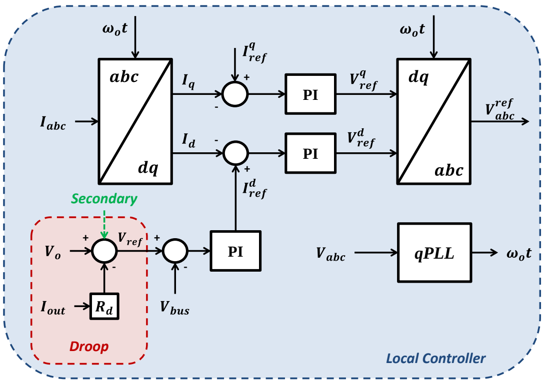

Figure 9. Front-end converter control diagram.

In the diagram of Figure 9, the output current I_{out} is considered as its DC-side current. The synchronous reference phase of the AC grid is obtained by a synchronous reference frame phase locked loop (qPLL), which has the three phase voltages V_{abc} as input signals.

It is relevant to observe that all controls were implemented in per unit quantities. The per unit realization in the primary and secondary controllers make the droop implementation more simple to calculate and to compare the control actions.

4 Simulation Results

In most of the scenarios the main test consists in the introduction of a constant power load on the main bus, connecting a 5 kW load in an instant of time. First, the behavior of the primary controllers is presented, demonstrating the effect of the line impedances in the system and the implementation of the front-end droop control strategy. And finally, the secondary action is analyzed in the system. The results will be analyzed with the presence of the line impedances of the cables.

4.1 Primary Control Action

Figure 10 shows the main bus voltage variations in each case in order to demonstrate the primary control behavior. The effect of the droop control strategy in the front end converter operating in the system is also analyzed in this section.

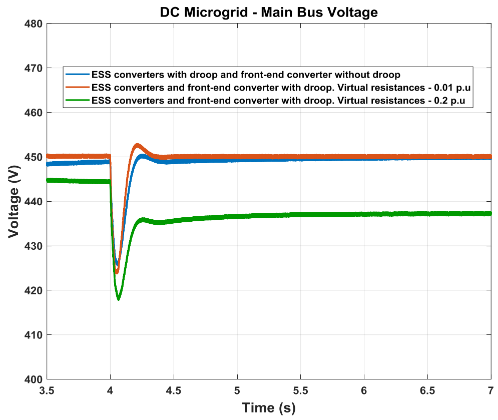

Figure 10. Main bus voltage comparison.

Figure 10 shows that, for both the cases with droop control only in the ESSs (blue line in Figure 10) and with droop control with virtual resistances of 0.01 p.u in both the front-end converters and the ESSs (red line in Figure 10), the bus voltage remains at nominal value (450 V) after the introduction of the constant power load at 4.0 seconds. This result demonstrates that the voltage regulation in steady state capability is increased with low droop values. On the other hand, Figure 11 and Figure 12 show that the power sharing between converters is not operating properly in both cases. Firstly, the power sharing when the droop control in the DC-AC converter is not operating is shown.

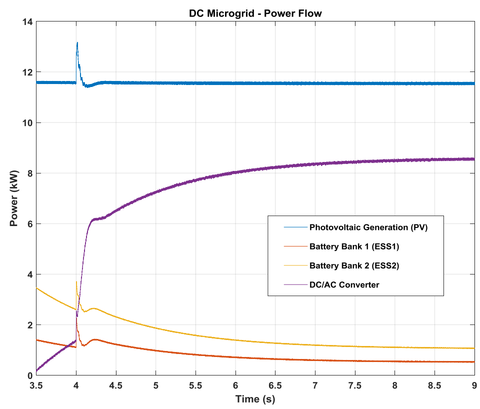

Figure 11. Power sharing – Front-end converter without droop control strategy.

It can be observed in Figure 11 that the front-end converter is assuming a great amount of the load in the system and the ESS converters are not contributing that much. This is caused by the inexistence of virtual impedance in the front end converter, which is trying to operate as an ideal voltage source. The transient regimen in this case is the slowest of all cases without secondary control. This denotes that the virtual resistance in the front end converter can also affect the transient performance.

Figure 12 shows that the power sharing between converters is not operating properly as well. The virtual resistances for this case are 0.01 p.u. Each virtual resistance is referred in the rated values of the respective converter shown in Table 1.

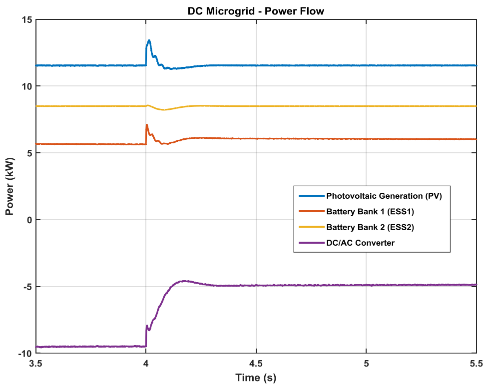

Figure 12. Power sharing - 0.01 p.u virtual impedances.

The power flow in the DC microgrid shown in Figure 12 demonstrates that both of the ESSs in the system have different values and the output power of the front-end converter is negative, meaning that the flow is from the DC bus to the AC utility grid. This characterizes an inconsistency, since the output power in two units that has the same rated power and the same virtual resistance should be equal. Furthermore, the output power of the front-end converter should be positive and bigger than the other units due to its rated power, respecting the proportional distribution of the load connected in the system. It is also possible to see that the power flow remains inconsistent before the constant load connection.

These operation conditions can be improved if the chosen virtual resistances of the droop control have higher values. Figure 13 present this scenario, where the virtual resistance of each converter is 0.2 p.u and the constant power load is connected at 4.0 seconds. The bus voltage is not working with its nominal value for the case when the droop control is implemented in the ESS and front-end converters operating with 0.2 p.u virtual impedances (see Figure 10).

When the constant load is inserted, the voltage level in steady state on the bus decreases after the transient response. This decrease in steady state indicates the load state of the microgrid. The higher value of the virtual resistances deteriorates the voltage regulation. However, the power mismatches in the system decreases.

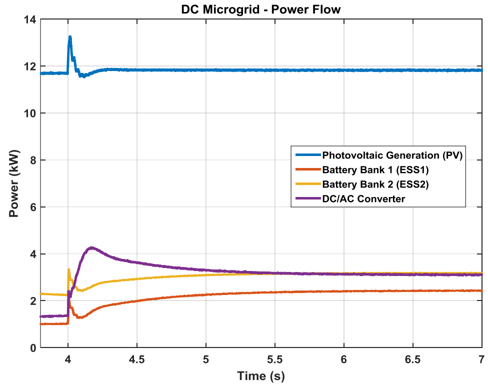

Figure 13. Power sharing - 0.2 p.u virtual impedances.

Figure 13 shows the power sharing in the microgrid. The DC-AC converter has a positive output power. This output power increases when the constant power load is applied. Nevertheless, there is a considerable power mismatch between ESS1 and ESS2 converters. This phenomenon is related with the line impedance differences in the system.

4.2 Secondary Control Action

In order to validate the secondary response methodology in the microgrid, a simulation case was planned to demonstrate its control action. The system starts operating with the constant power load, and the secondary control starts to act in 4.0 seconds. The virtual resistance in primary control is the same in p.u for each converter and is equals to 0.1 p.u.

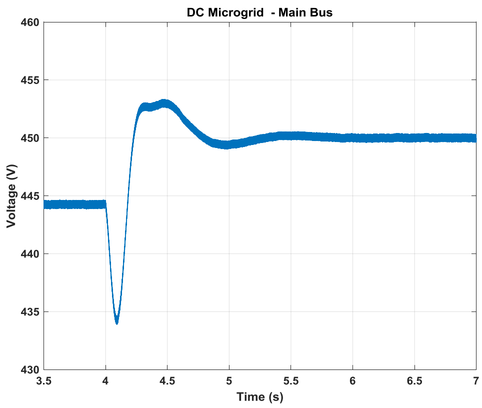

Figure 14. Secondary control action in the bus voltage.

Figure 14 presents the bus voltage behavior with the secondary control effort. In this case, the front-end converter and ESS1 converter have the bus voltage regulation strategy (V_{sv}) while ESS2 has the current compensation strategy (V_{si}). Before the secondary control order, the bus voltage is operating near 445 V, with all loads already connected. When the simulation time reaches 4.0 seconds, a transient state starts and the bus voltage increases to 450 V. An undershoot is perceptible in the transient response of the bus voltage, even though no loads are connected in this moment. This undershoot is inherent to the power transient of the converters.

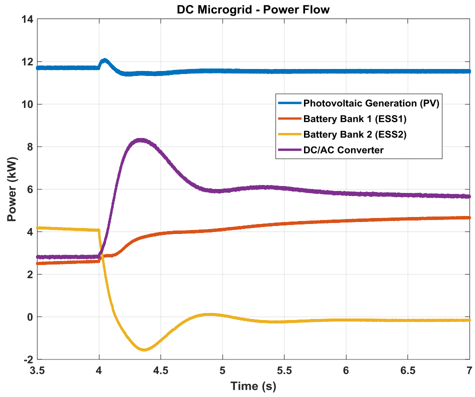

Figure 15. Secondary response in the microgrid power flow.

Figure 15 illustrates the power flow in the microgrid for this case. When the secondary controllers begin, the output powers of DC-AC converter and ESS1 start to rise in order to increase the bus voltage. In contrast, the output power of ESS2 decreases to achieve the accurate point of its output current. When the bus voltage is 450 V, the output power of ESS2 is about zero. This variation occurs due to the droop curve and the secondary law in this converter. When the voltage is fully regulated, the result of the equation (12) is ideally zero for an ESS unit. Then the secondary control actuates to decrease the output power, causing the undershoot in Figure 14. In steady state the front-end converter has the higher output power, denoting a proper power sharing. The dynamics of the system are slower in this scenario. This is expected since the secondary control order must be slower than the primary control order.

5 Conclusions

In this paper, a hierarchical control adapting a droop technique in a front-end DC-AC converter was implemented to a DC microgrid. The control scheme of primary and secondary control was performed and evaluated.

Observing the simulation scenarios, it is possible to conclude that the hierarchical structure is effective, and allows power mismatches minimization considering line impedances, increasing the flexibility and reliability of the control system. The primary control of the front-end converter using synchronous frame reference was validated as an effective strategy to implement the droop control law in DC-AC converters. In addition, it was demonstrated that the droop control methodology applied in the front end converter can operate in a DC microgrid that contains different elements, like DGs and ESS units.

Future works will be done implementing the tertiary control, to enhance the system strategies and implement algorithms capable to optimize the operation of the energy storage systems in the DC microgrid.

References

Chen, F., Burgos, R., Boroyevich, D., Zhang, W., (2015). A nonlinear droop method to improve voltage regulation and load sharing in DC systems. 2015 IEEE 1st International Conference on Direct Current Microgrids, ICDCM 2015 45–50.

Chen, F., Zhang, W., Burgos, R., Boroyevich, D., (2014). Droop voltage range design in DC micro-grids considering cable resistance. 2014 IEEE Energy Conversion Congress and Exposition, ECCE 2014 770–777.

Dragicevic, T., Lu, X., Vasquez, J.C., Guerrero, J.M., (2016). DC Microgrids - Part I: A Review of Control Strategies and Stabilization Techniques. IEEE Transactions on Power Electronics 31, 4876–4891.

Iravani, R., Khorsandi, A., Ashourloo, M., Mokhtari, H., (2016). Automatic droop control for a low voltage DC microgrid. IET Generation, Transmission & Distribution 10, 41–47.

Jin, C., Wang, P., Xiao, J., Tang, Y., Choo, F.H., (2014). Implementation of hierarchical control in DC microgrids. IEEE Transactions on Industrial Electronics 61, 4032–4042.

Meng, L., Shafiee, Q., Trecate, G.F., Karimi, H., Fulwani, D., Lu, X., Guerrero, J.M. (2017). Review on Control of DC Microgrids and Multiple Microgrid Clusters. IEEE Journal of Emerging and Selected Topics in Power Electronics 5, 928–948.

Ott, L., Han, Y., Wunder, B., Kaiser, J., Fersterra, F., Schulz, M., Marz, M. (2015). An advanced voltage droop control concept for grid-tied and autonomous DC microgrids, in: 2015 IEEE International Telecommunications Energy Conference (INTELEC). IEEE, pp. 1–6.

Prieto-Araujo, E., Bogdan Bolboceanu, D., Sanchez-Sanchez, E., Gomis-Bellmunt, O., (2017). Design methodology of the primary droop voltage control for DC microgrids, in: 2017 IEEE Second International Conference on DC Microgrids (ICDCM). IEEE, pp. 529–535.

Tremblay, O., Dessaint, L. -a., Dekkiche, A.-I., (2007). A Generic Battery Model for the Dynamic Simulation of Hybrid Electric Vehicles. 2007 IEEE Vehicle Power and Propulsion Conference 284–289.

Xiao, J., Wang, P., Setyawan, L., (2015). Hierarchical Control of Hybrid Energy Storage System in DC Microgrids. IEEE Transactions on Industrial Electronics 62, 4915–4924.

Zheng, Z., Wang, X., Li, Y., (2011). A control method for grid-friendly photovoltaic systems with hybrid energy storage units. 2011 4th International Conference on Electric Utility Deregulation and Restructuring and Power Technologies (DRPT) 1437–1440.